Optical and Quantum Electronics (2022) 54:755
https://doi.org/10.1007/s11082-022-04189-3

One-dimentional periodic structure infiltrated by (PVA/CV + CF)-polymer for high-performance sensitivity

Fatma A. Sayed[1] · Hussein A. Elsayed[1] · Ahmed Mehaney[1] · M. F. Eissa[1] · Arafa H. Aly[1]

Received: 30 June 2022 / Accepted: 7 September 2022 / Published online: 27 September 2022

Abstract
In the current work, we demonstrate a design to act as a Gamma-ray radiation dosimeter based on the one-dimensional photonic crystal (1D-PhC). The basic concept of the present dosimeter is based on a Porous Silicon (PSi) infiltrated by poly-vinyl alcohol (PVA)-polymer doped with crystal violet (CV) and carbol-fuchsine (CF) dyes. The mechanism of suggested dosimeter is based on the shift of the photonic bandgap (PBG) to higher wavelengths as exposed to gamma-ray radiation doses from 0 to 70 Gray (Gy). The basic axes of the current theoretical treatment are the transfers matrix method (TMM), Bruggeman's effective medium equation, and the fitted experimental data to the refractive index of the doped PVA-Polymer. The obtained results showed the proposed sensor is characterized by high stable sensitivity varied from (178–186 nm/ RIU) along an applied γ-dose from (10–70 Gy) in the visible range. In addition, we compared these results with previous researches. In addition, based on the our knowledge may be it is the first time that a 1D-PhC has been used for gamma-ray detection by using (PVA/CV + CF) based on Porous Silicon.

Keywords Polymers · Photonic crystals · Porous silicon · Radiation dosimeters · Gamma-ray radiation · Transmittance spectra · Transfer matrix method

1 Introduction

Radiations of varied degrees cause and induce many Physico-chemical changes in the materials that come into contact with them in the environment. Radiations influence various materials by varying degrees, depending on the type of radiation, radiation dosage level, exposure time, material characteristics, environmental conditions, etc. (Chandrappa et al. 2021; Aly et al. 2015). Radiation dosimetry is the main point of much research due to the use of radiation in various applications(Baccini, et al. 2019; Andreo, et al. 2017). A dosimeter is any instrument that can produce an output value that represents the average absorbed dose deposited in its sensitive volume by ionizing radiation(Baccini, et al. 2019;

✉ Arafa H. Aly
arafa.hussien@science.bsu.edu.eg

[1] TH-PPM Group, Physics Department, Faculty of Sciences, Beni-Suef University, Beni Suef, Egypt

Chu, et al. 2008). What's needed is a system that's simple to be used and set up, and that can detect radiation in real-time and from far distances. It also needs to be long-lasting and cost-effective.

Polymers with excellent surface and bulk properties have grown in relevance significantly over the last few decades due to their low weight, low cost, easy processability, and ease of fabrication of thick and thin samples. PVA (Poly-Vinyl Alcohol) is a polymeric substance with a wide range of applications. This is due to their great optical properties, lightweight, and mechanical properties, as well as the fact that they are an excellent host material for composites(Hadi Al-kadhemy et al. 2014; Ali Omer and Ali Bashir 2018). Most PVA works have composites that are sensitive to low or high-energy radiations, resulting in improved or degraded physicochemical qualities (Chandrappa et al. 2021; Hadi Al-kadhemy et al. 2014; Ibrahim et al. 2021; Mir et al. 2016; Sharaf et al. 1995; Al-Kadhemy and Abass 2013; Raghuvanshi et al. 2012; Antar 2014).

When high-energy radiation (i.e., X-rays, γ-rays, etc.) interacts with polymeric materials, it causes chain scission. This results in a decrease in molecular weight, and inter/intermolecular cross-linking. This also results in an increase in molecular weight, emission of atoms, molecules, and molecular fragments, free radical formation, and the production of reactive oxygen species (ROS). All of this eventually leads to degradation, color change, brittleness, hardness, etc. Where, the optical, thermal, mechanical, dielectric, and conductivity properties of radiation-exposed composite materials could be fine-tuned as a result of these structural alterations (Chandrappa et al. 2021; Raouafi et al. 2018). Many scientists have been studying the impact of irradiation on doped polymer composite materials to investigate their unique features (Hadi Al-kadhemy et al. 2014; Ali Omer and Ali Bashir 2018; Al-Kadhemy and Abass 2013).

Gamma-Ray radiation dosimetry at the micro and the nanoscale is required for medical and industrial applications such as microbeam radiation treatment, microelectronics, and radio-synthesis of nanomaterials(Archer et al. 2019; Chmielewska 2017; Zimek 2017). Different techniques, such as the oscillometric readout method, the Gafchromic method, the spectrophotometric readout method, and optical methods, can be used to determine the gamma-ray radiation dose (Ibrahim et al. 2021). Based on the radiation effects, the optical approaches for radiation dose monitoring can be divided into four types. The first type is based on the radiation-induced luminescence and thermoluminescence effect (Ali Omer and Ali Bashir 2018; Rozaila et al. 2016; Afifi 2021). The second type is based on the radiation-induced attenuation (RIA) effect (Cai et al. 2017; Kashaykin et al. 2019; Kashaykin et al. 2015). The third type is based on varying the frequency of the Brillouin scattering in the distributed optical fibers (Alasia, et al. 2005). The final type is based on photonic crystal fiber and Bragg gratings structures (Baccini, et al. 2019). Photonic crystals (PhCs) have recently gained prominence in a variety of applications such as optical fibers, sensors, and biomedical devices (Entezam et al. 2016; Elsayed et al. 2021; Sayed et al. 2022). Photonic band gaps (PBGs) are a key and unique feature of PhCs that prevent light from propagating at particular frequency intervals, which come from destructive interference of the PhC's constituent materials. Reference (Bijalwan et al. 2021) study the sensing performance of a one-dimensional photonic crystal (PC) based sensor for the detection of blood plasma and cancer cells. Reference (Abohassan et al. 2021) create an effective sensor based on a one-dimensional binary photonic crystal for detecting the fat content in commercial milk. Reference (Qutb et al. 2021) using a 1D-defective photonic crystal structure, show the sensing concept for concurrently detecting the salinity and temperature of seawater. Reference (Sabra, et al. 2022) In the mid-IR range, the 1D-PhC was introduced as an optical pressure sensor.

Polymers, metals, semiconductors, liquid crystals, superconductors, metamaterials, and dielectrics are all utilized in the design of PhCs (Hadi Al-kadhemy et al. 2014; Elsayed et al. 2021; Wu 2021; Iwamoto et al. 2021; Park et al. 2021). The incorporation of porous silicon (PSi) layers in PhCs as a novel sensor design to improve sensitivity is the focus of recent research (Ivanov et al. 2022; Van 2022). PSi layer is commonly fabricated by an electrochemical etching route. Due to its simplicity of manufacture, different pore sizes and morphologies, vast surface area, and controlled surface modification and reactivity, it is highly recommended and considered to be a promising candidate (Al-Syadi et al. 2021; Yue et al. 2019; Zhong et al. 2020; Zaky and Aly 2021).

In this work, we develop a highly sensitive radiation dosimeter; 1D-PhC based on PSi layers infiltrated by PVA-polymer doped with crystal violet (CV) and carbol fuchsine (CF) dyes. Also, we studied the behavior of this structure when exposed to different doses of gamma rays emitted from a ^{60}Co-radioactive source. In addition, the results show how the PSi-layer enhanced the optical properties of the doped PVA-Polymer, and how the porosity of PSi-layers affects our structure. Then, the effect of gamma-ray doses ranging from 0 to 70 Gy on our structure is studied. Finally, the effect of thicknesses of the two layers on our structure and how much they affect the sensitivity of this radiation-dosimeter are discussed.

2 Theoretical framework

In this part, we design a gamma-ray dosimeter by a 1D-PhC based on the Porous Si layer. As shown in Fig. 1, the structure is configured as [Air $(PSi_1/PSi_2)^{N}{}_1$ substrate]. Where, PSi_1, PSi_2 are the first and second porous silicon layers with porosity P_1, P_2, respectively, and N_1 represents the number of periods. For gamma-ray detection, we used PSi-layer to be infiltrated by the doped PVA-Polymer. The transfer matrix method (TMM) is used to study the transmittance spectra of our structure (Ahmed and Mehaney 2019; Aly and Sayed 2020; Aly et al., 2009; Aly and Mohamed. 2015).

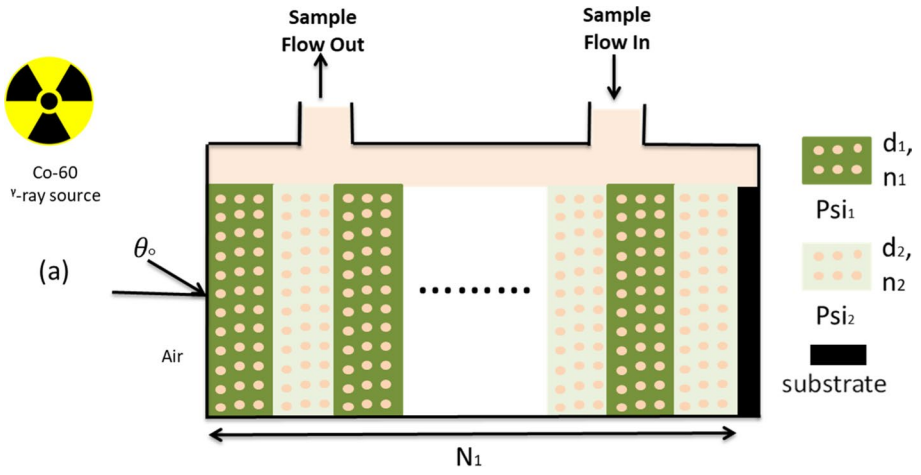

Fig. 1 Schematic diagram of a 1D-Binary PhC gamma-ray dosimeter. The structure of 1D-PhC is surrounded by air and glass substrate and the number of periods = 20

As a result, the Porous Silicon layer, the doped PVA-Polymer, and the transfer matrix method are the main points to illustrate our theoretical study.

2.1 Optical properties of the porous silicon layer

The optical refractive index of the PSi layer (n_{PSi}) that is filled with Polymer ($n_{Polymer}$) with porosity (P) is calculated using Bruggeman's effective medium equation (Zaky and Aly 2021; Ahmed and Mehaney 2019).

$$n_{(PSi)} = 0.5\sqrt{\in + \varphi} \tag{1}$$

$$\epsilon = 3P\left(n_{(Polymer)}{}^2 - n_{(Si)}{}^2\right) + \left(2n_{(Si)}{}^2 - n_{(Polymer)}{}^2\right) \tag{2}$$

$$\varphi = \sqrt{\epsilon^2 + (8^2 n_{(Si)}{}^2 n_{(Polymer)}{}^2)} \tag{3}$$

where, $n_{(Si)}$ is the refractive index of the silicon, and is equal to 3.7 (Elsayed et al. 2021).

2.2 Optical properties of the PVA-polymer

The film samples of the (PVA/CV + CF) polymer were prepared by using a solvent casting method. These films were irradiated At room temperature with gamma-ray doses of 0–70 (Gy) emitted from ^{60}Co-source (Antar 2014).

The refractive index of the (PVA/CV + CF) polymer is given as a function of wavelength and gamma-ray radiation doses D_γ (Gy) by fitting the experimental results using the Matlab program (Antar 2014). Applying the cubic fitting to the experimental data, the following fitted equations can be used to express the refractive index of the polymer as follows.

$$n(D) = A\lambda^3 + B\lambda^2 + C\lambda + D \tag{4}$$

where, A, B, C, and C are the fitted coefficients and are listed in Table 1. The R-square value of the fitting is equal that the value of 0.015963 through gamma-ray radiation doses ranging from 0 (unirradiated sample) to 70 Gy.

Table 1 Constants of the refractive index of the (PVA/CV + CF)-Polymer are given as a function of wavelength at different gamma-ray doses (Gy)

D_γ (Gy)	A	B	C	D
0	1.7479×10^{-7}	−0.00025167	0.11796	−15.571
10	1.5689×10^{-7}	−0.00022845	0.1083	−14.282
20	1.3002×10^{-7}	−0.00019042	0.090693	−11.606
30	1.2167×10^{-7}	−0.00017806	0.084739	−10.663
40	1.0444×10^{-7}	−0.00015298	0.07293	−8.87
50	1.013×10^{-7}	−0.00014864	0.070913	−8.5343
60	9.754×10^{-8}	−0.00014305	0.068283	−8.1388
70	9.6042×10^{-8}	−0.00014056	0.067049	−7.9382

2.3 Transfers matrix method (TMM)

The transfer matrix method (TMM) is used to determine the optical properties of the presnt structure (transmittance, reflectance, and absorbance spectra) because of electromagnetic waves interaction with our structure. Many previous studies have investigated the details of TMM (Elsayed et al. 2021; Sayed et al. 2022; Zaky and Aly 2021; Aly et al. 2022; Abadla et al. 2021; El-Shemy et al. 2022; Mehaney et al. 2019; Mehaney 2019). The following matrix (M) represents the total transfer matrix for the proposed structure with the number of periods (N_1) of PSi_1 and PSi_2-layers:

$$M = (M_{PSi_1} M_{PSi_2})^{N_1} = \begin{pmatrix} m_{11} & m_{12} \\ m_{21} & m_{22} \end{pmatrix} \tag{5}$$

Then, the transmittance spectra of our structure could be described according to the previous matrices as: -

$$T = \frac{P_s}{P_o}|t|^2 = \frac{2P_o}{(m_{11} + m_{12}P_s)P_o + m_{21} + m_{22}P_s} \tag{6}$$

where, P_o, P_s are the propagation matrix of air and substrate for TE-polarization, respectively.

3 Results and discussion

Herein, the numerical results of our 1D-PhC gamma-ray dosimeter based on PSi-layer are discussed in this section. These results include the transmittance spectra of our structure in the visible region for a transverse electric (TE) polarization. The refractive indices of Si, air and glass are $n_{Si} = 3.7$, $n_{Air} = 1$, and $n_s = 1.52$, respectively (Zimek 2017). The refractive index of the PSi and Polymer are mentioned in Eqs. (1) and (4). By injecting the polymer at the top of the structure, the pores will be infiltrated with the polymer as shown in Fig. 1. The thickness of the first layer (PSi_1) and the second layer (PSi_2) are $d_1 = 30$ nm, and $d_2 = 73$ nm with porosity of $P_1 = 20\%$, $P_2 = 80\%$, respectively. Furthermore, the period of numbers is $N_1 = 20$.

The first point in this section explains the effect of radiation on the dimension of our radiation dosimeter and the reason for choosing these materials. The radiation damage is critical for devices that operate in radiation-prone environments. Wherein, radiation dosimeters are exposed to pressure, temperature, or strain from external sources during Gamma-radiation. The reason behind choosing Si material is that the refractive index of Si changes below (5×10^{-5}) at ($D\gamma = 1000$ kGy). Also, the thermo-optic coefficient of Si is equal (2.3×10^{-4}) at ($D\gamma = 66.5$ kGy, and 32 °C) (Baccini, et al. 2019; Cocorullo et al. 2002). And the maximum rise in the temperature of Si is equal to (3.2 °C) due to the radiation effect. Besides, the thermal expansion coefficient of the Si is very small and equals ($\approx 2.6 \times 10^{-6}$)(Okada and Tokumaru 1984). Therefore, the change in the refractive index of Si caused by the radiation processes across a γ-dose range from 0 to 70 Gy can be ignored. Additionally, the effect of radiation on the geometrical dimensions (thermal expansion) of the proposed sensor (radiation dosimeter) is ignored. The thermal strain caused by radiation can thus be ignored (Ibrahim et al. 2021). To sum

up, we think the proposed structure is suitable for measuring gamma rays without being destroyed.

For, the effect of radiation on the refractive index of the (PVA/CV + CF) polymer is shown in Fig. 2. The fitting of the experimental results examined in reference(Antar 2014) is discussed in this figure. Based on this figure, the fitting parameters in Table 1 are calculated. Through the varied values of Dγ (Gy), the figure demonstrates a sufficient matching with the experimental results. This indicates that the fitting process produces the same results as the experimental data, and the fitting parameters are suitable for calculating the (PVA/CV + CF) polymer's refractive index.

Figure 2, shows the (PVA/CV + CF) refractive index for unirradiated and irradiated polymer in the range (10–70 Gy) γ-ray doses from wavelength 380 nm to 550 nm. The refractive index reduces gradually as the wavelength increases, and the changes become larger as the wavelength increases. Whereas crystallization, density, electronic structure, and defects are all potential causes for changes in the refractive index induced by γ-radiation (Antar 2014). The refractive index increases with doses of irradiation, as shown in Fig. 2; for example, when doses irradiation increases from 0 to 70 Gy, the n changes from 2.24 to 2.40 at the wavelength (λ = 555 nm). The increase in the polymer's refractive index after irradiation could be due to ionization, and/or atomic displacements caused by a gamma-ray collision with the samples, which could alter the internal structure of the polymer films (Antar 2014).

Figure 3, shows the effect of the porous silicon on the refractive index of the doped polymer (PVA/CV + CF), and the effect of porosity on the refractive index of the porous silicon infiltrated by the doped polymer [PSi $_{(PVA/CV+CF)}$]. As shown in Fig. 3a, the porous silicon material enhanced the refractive index of the doped polymer [n (PSi $_{(PVA/CV+CF)}$)]. Indeed, the refractive index increased from 2.53 to 2.82 at λ = 400 nm, and from 2.25 to 2.63 at λ = 560 nm, respectively. According to Bruggeman's effective-medium approximation as Eq. (1), the refractive index of porous silicon depends on the refractive index of silicon and the refractive index of the material inside the pores. So, any change in the refractive index of the material inside the pores, reflects on the refractive index of porous silicon material. This is the essential point on which our gamma-ray dosimeter is based. Whereas any change in the refractive index of doped polymer induced by γ-radiation will reflect on the refractive index of the material. In addition, the refractive index of porous silicon depends on the porosity value, as shown in Eq. (1). Figure 3b, shows the dependence of the refractive index of [PSi $_{(PVA/CV+CF)}$] on the variation of porosity. The refractive index of [PSi $_{(PVA/CV+CF)}$] decreases with an increase

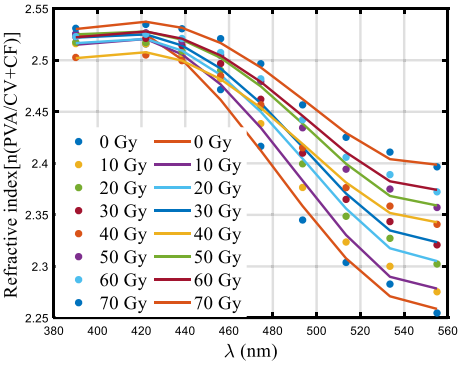

Fig. 2 The response of the refractive index of PVA-Polymer doped with CV + CF to the Gamma-Ray radiation variation based on the fitting of the experimental data(Antar 2014)

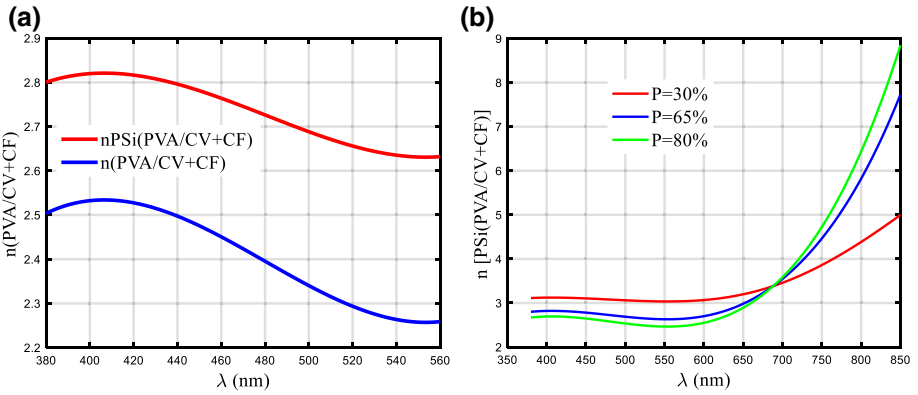

Fig. 3 **a** The difference between the refractive index of (PVA/CV + CF) and refractive index of PSi (PVA/CV + CF) at zero Gy, with a Porosity of 65%. **b** The Effect of Porosity on the refractive index of [$PSi_{(PVA/CV+CF)}$] at zero Gy

in the porosity value from λ = 350 nm to λ = 690 nm, then increases with an increase in the porosity value for λ > 690 nm. The refractive index equals 3.12, 2.82, and 2.69 for $P = 30\%$, 65%, and 80% at λ = 400 nm. Figure 4, shows the effect of γ-doses in the range (0–70 Gy) on the refractive index of [$PSi_{(PVA/CV+CF)}$] with porosity equal to 65%. The refractive index firstly slightly increases with the increase in the γ-ray doses and then decreases with the increase in the γ-ray doses in all wavelength ranges.

Figure 5, represents the transmittance spectra of our proposed structure of the gamma-ray dosimeter for TE-modes calculated by the TMM method. The initial geometrical parameters of this structure are set as $d_1 = 30$ nm, and $d_2 = 73$ nm with porosity $P_1 = 20\%$, and $P_2 = 80\%$, respectively, and $N_1 = 20$. The photonic bandgap (PBG) appears in the visible range with the left side wavelength ($\lambda_L = 527.5$ nm), right side wavelength ($\lambda_R = 678.7$ nm), and the width of PBG equal ($\Delta\lambda = \lambda_L - \lambda_R = 151.2nm$). The principle behind this structure is that the PBG works as a sensor for gamma-ray radiation. When the structure is exposed to gamma-ray radiation, the refractive index of materials will be changed and then the PBG will change as well. Before showing the effect of gamma-ray radiation on the PBG, we are doing optimization for the parameters of this structure.

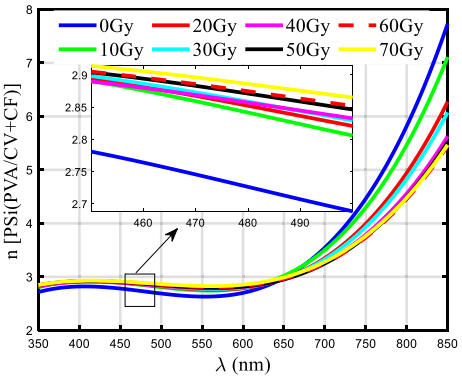

Fig. 4 The effect of the gamma-ray radiation on the refractive index of [$PSi_{(PVA/CV+CF)}$] at a porosity of 65%

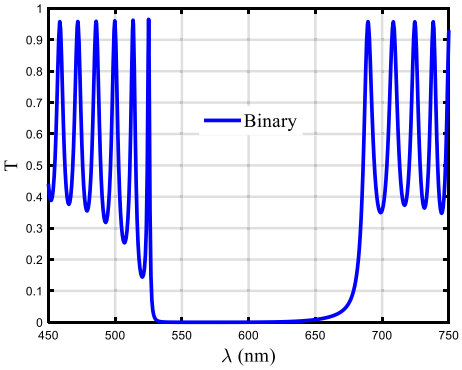

Fig. 5 Transmittance spectra of 1D-Binary structure with thickness $d_1 = 30$ nm, $d_2 = 73$ nm, N-period = 20, and porosity of $P_1 = 20\%$, $P_2 = 80\%$ at zero gamma-ray radiation

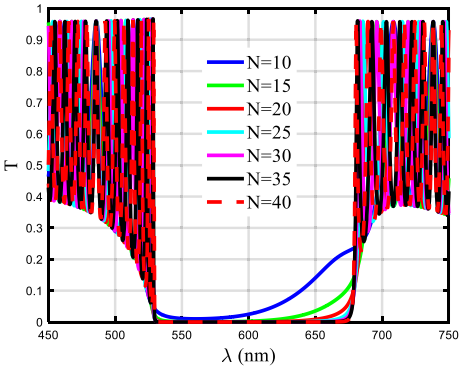

Fig. 6 Transmittance spectra of 1D-Binary structure with thickness $d_1 = 30$ nm, $d_2 = 73$ nm, and porosity $P_1 = 20\%$, $P_2 = 80\%$ at zero gamma-ray radiation at different N-period

Figure 6, shows the transmittance spectra of our structure at the different number of periods. We note that the PBG became sharper and steeper as the number of periods increased. In addition, there is no change in the transmission spectra of this structure, and the width of the PBG doesn't affect by increasing the number of periods. In other words, we choose $N_1 = 35$ in the following calculation to the PBG become more suitable for the detection of gamma-ray radiation.

Figure 7, shows the effect of porosity of the first and the second layer of our structure on the PBG sensor. As shown in Fig. 7a, b with the increase in the porosity of the first layer (P_1) and the second layer(P_2), the width of the PBG decreases. We choose $P_1 = 30\%$ and $P_2 = 85\%$ for the width of the PBG to appear in a wide and suitable form. Because the primary focus of this study is on the development of radiation-resistant FBGs for use in nuclear environments in temperature and strain measurement applications.

Now, we show the effect of γ-doses (Gy) from (0–70 Gy) on the PBG sensor of our radiation dosimeter, as shown in Fig. 8a. It can note that with an increase in the value of γ-doses (Gy), the left side of the PBG shifts to a higher wavelength, and the width of the PBG is affected by this radiation. This shift is due to the change in the refractive index of the Psi-layer which is induced by gamma-ray radiation.

We examine the performance of our radiation dosimeter by calculating the sensitivity of the dosemeter. The sensitivity (S) is defined as the difference in the wavelength ($\Delta\lambda_L$)

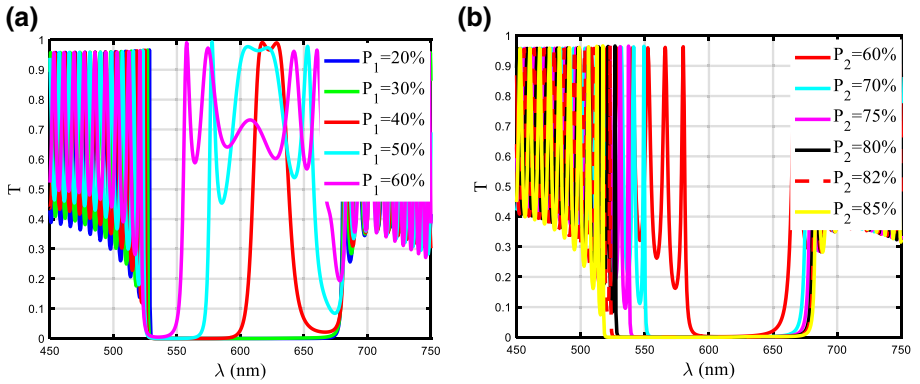

Fig. 7 The effect of the porosity on the photonic bandgap of our design for TE at $d_1 = 30$ nm, $d_2 = 73$ nm, N = 35, at zero gamma-ray radiation. **a** For the porosity of the first layer, **b** For the porosity of the second layer

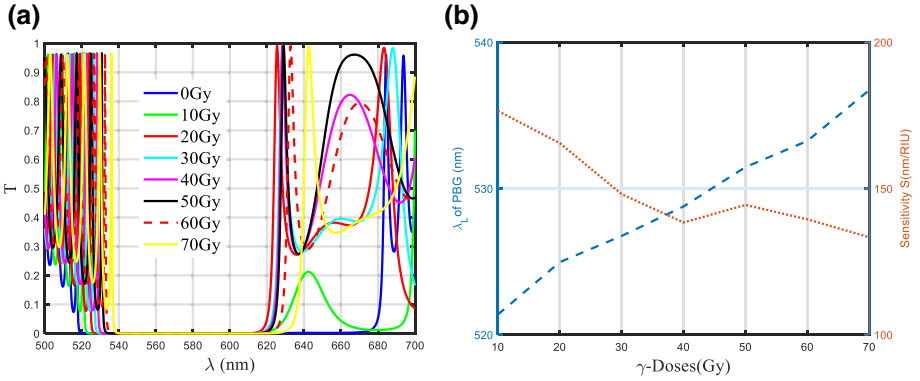

Fig. 8 **a** The effect of gamma-ray radiation on transmittance spectra of our structure with a thickness of $d_1 = 30$ nm, $d_2 = 73$ nm, porosity $P_1 = 30\%$, $P_2 = 85\%$, and N-Period = 35. **b** The left edge side of PBG and the sensitivity at different γ-doses (Gy) from (0–70 Gy)

to the difference in the refractive index of doped PVA-polymer and units of (nm/RIU), as the following Eq. (7).

$$S = \frac{\Delta \lambda_L}{\Delta n_{(Polymer)}} \tag{7}$$

Figure 8b, shows the effect of γ-doses (Gy) on the left band side of the PBG (λ_L) and the sensitivity of this radiation dosimeter. We noted that with an increase in γ-doses from (10 Gy) to (70 Gy), the (λ_L) an increase from (521.3 nm) to (536.7 nm), and the sensitivity decrease from (176.5 nm/RIU) to (133.3 nm/RIU). We will study the geometrical parameters that will maximize the shift of the PBG's left band side, and therefore sensor sensitivity, under various radiation doses. The effect of thickness of the first layer PSi_1 with values of (33, 35, 38, and 40 nm) at different γ-doses (Gy) on the PBG and sensitivity of this will be studied, while the other parameters are kept constant. As shown in Fig. 9a, b, c, and d,

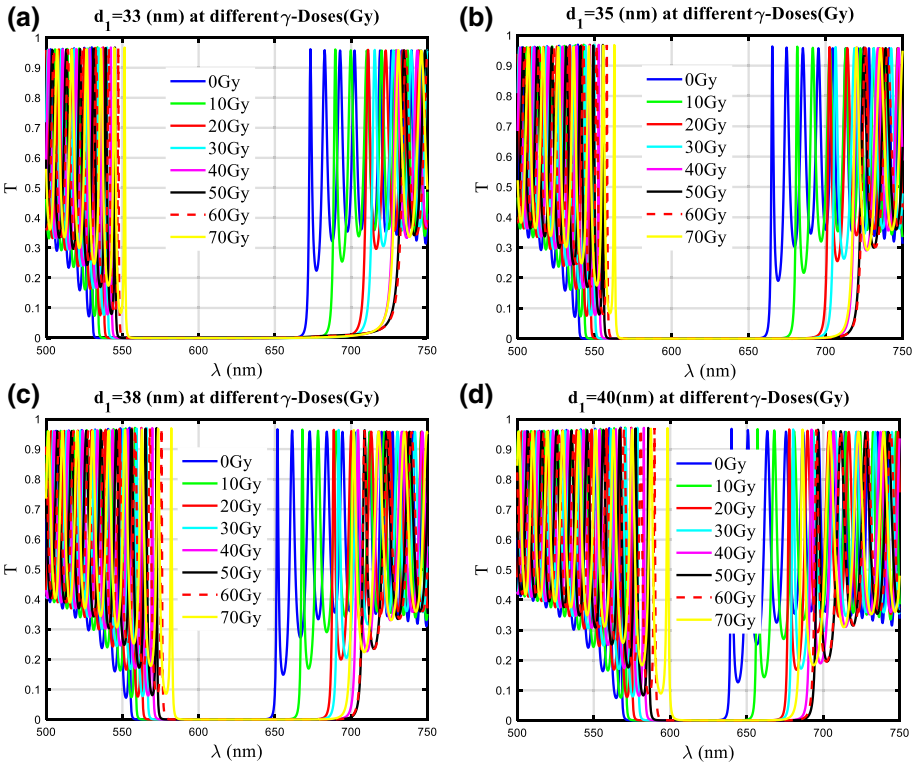

Fig. 9 The effect of the thickness of first layer $PSi_{1\ (PVA/CV+CF)}$ on the properties of our design for TE at $d_2 = 73$ nm, $N_1 = 35$, and porosity $P_1 = 30\%$, $P_2 = 85\%$ at γ-doses (Gy) from (0–70 Gy)

generally, it noted that with an increase in the thickness of the first layer, the left side of the PBG an increase and shift to longer wavelengths at the same value of γ-dose (Gy). Eg; At γ-dose is equal (10 Gy), with an increase of d_1 (33, 35, 38, and 40 nm), the (λ_L) increase with values (534.3, 543.5, 559.1, and 571.6 nm), respectively. In addition, at each value for this thickness, we study the effect of γ-doses (Gy), and we noted that the (λ_L) shifted

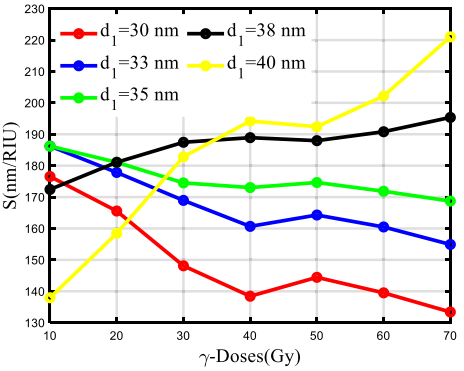

Fig. 10 The effect of the thickness of first layer $PSi_{1\ (PVA/CV+CF)}$ on the sensitivity of our design for TE at $d_2 = 73$ nm, $N_1 = 35$, and porosity $P_1 = 30\%$, $P_2 = 85\%$ at γ-doses (Gy) from (0–70 Gy)

to higher wavelengths with an increase in the value of γ-doses (Gy). Then, we study the sensitivity of the different thicknesses of the first layer at different γ-doses (Gy), as shown in Fig. 10. We conclude from Fig. 10 that, when the thickness of the first layer equals the value of 38 nm, our radiation dosimeter gives sensitivity with very high stability and equals ≈195 nm/RIU. Consequently, the thickness of the first layer is taken as 38 nm.

Secondly, we study the effect of the thickness of the second layer PSi_2 with values (72, 74, 76, and 77 nm) at different γ-doses (Gy) on the PBG and the sensitivity of this radiation dosimeter. The effect of the thickness of the second layer gives the same behavior as the first layer. As shown in Fig. 11a, b, c, and d, at γ-dose is equal (10 Gy), with an increase of d_2 (72, 74, 76, and 77 nm), the (λ_L) increase with values (554.6, 563.9, 575.1, and 581.6 nm), respectively. With an increase in the value of the γ-doses (Gy) at each value of the thickness of the second layer, the (λ_L) shifted to higher wavelengths. The sensitivity at each thickness of the second layer and at different values of the γ-doses (Gy) was studied as shown in Fig. 12. We note that at each value of the thickness of the second layer, with the increase in the value of the γ-doses (Gy), the sensitivity gradually increases. When the thickness of the second layer equals the value of 72 nm, the sensitivity is characterized by very high stability at each of the applied γ-doses (Gy) and equals ≈186 nm/RIU. Therefore, the thickness of the second layer is taken as 72 nm.

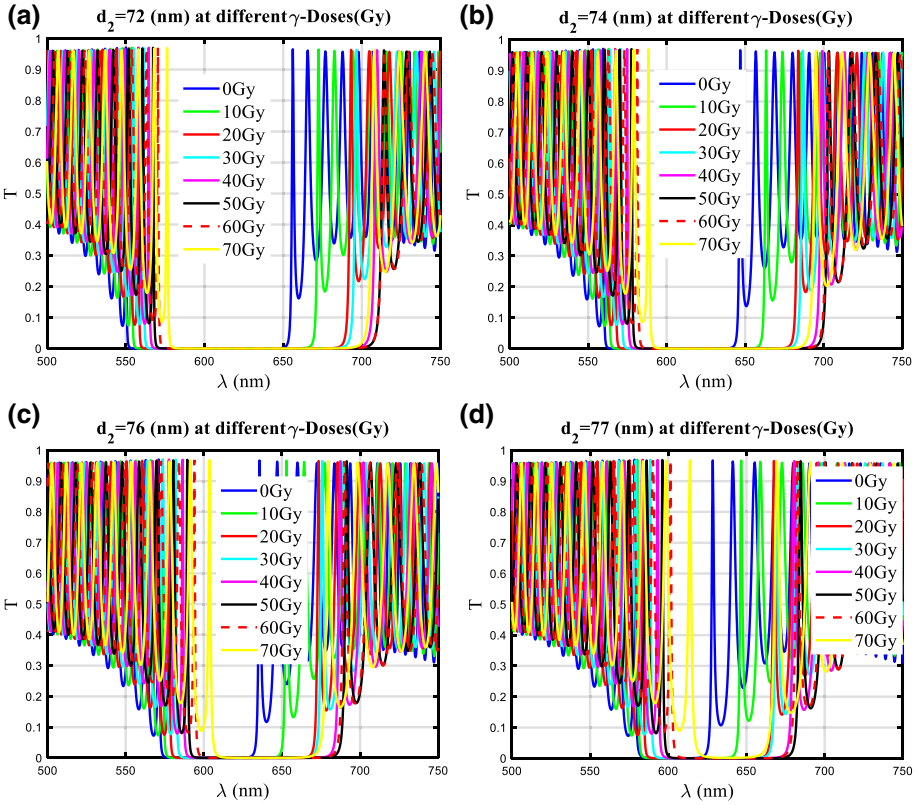

Fig. 11 The effect of the thickness of second layer $Psi_{2\ (PVA\text{-}Polymer)}$ on the properties of our design for TE at $d_1 = 38$ nm, N = 35, and porosity of $P_1 = 30\%$, $P_2 = 85\%$ at γ-doses (Gy) from (0–70 Gy)

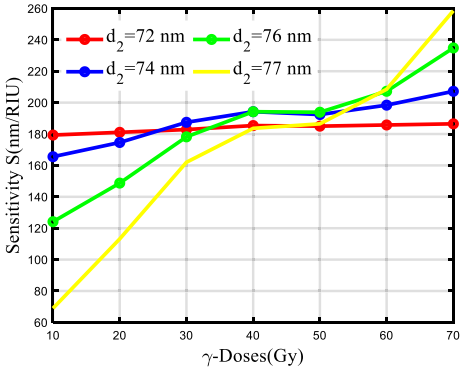

Fig. 12 The effect of the thickness of second layer $Psi_{2(PVA\text{-}Polymer)}$ on the sensitivity of our design for TE at $d_1 = 38$ nm, N = 35, and porosity $P_1 = 30\%$, $P_2 = 85\%$ at γ-doses (Gy) from (0–70 Gy)

The relation between the left side of the PBG and the γ-doses (Gy), in addition to the relation between the sensitivity and the γ-doses (Gy) at the optimized parameters, is given by the following equations based on the data fitting in the form of the 4th-degree polynomial:

$$S = 3.7062 \times 10^{-6} {D_\gamma}^4 - 0.00058481 D_\gamma^3 + 0.029151 D_\gamma^2 - 0.36176 D_\gamma + 180.6,$$

$$\mathrm{R} = 0.84006 \tag{8}$$

$$\lambda_L = 2.4793 \times 10^{-6} {D_\gamma}^4 - 0.00029159 D_\gamma^3 + 0.0094989 D_\gamma^2 + 0.29031 D_\gamma + 550.99,$$

$$1\mathrm{R} = 0.84006 \tag{9}$$

Finally, a comparison between our study and previous experimental radiation dosimeter used is shown in Table 2. This table shows firstly the proposed gamma-ray dosimeter based on 1D-photonic crystals and using porous silicon layers is a unique study and did not exist before. Furthermore, this radiation dosimeter achieved the highest sensitivity of 186 nm/RIU compared to published results in this part with very stability along the range of visible wavelengths when the design is exposed to gamma-ray doses from 0 to 70 Gy.

4 Conclusion

We developed a highly sensitive 1D-PhC radiation dosimeter based on PSi-layers infiltrated by PVA-polymer doped with crystal violet (CV) and carbol fuchsine (CF) dyes. The theoretical analysis is investigated by fitting the experimental data of the doped PVA-polymer, the Bruggeman's effective medium equation of PSi-layer, and the transfer matrix method for calculating the optical properties of the dosimeter structure. The numerical results demonstrated that the PSi-layers enhanced the refractive index of the doped PVA-Polymer. In addition, they illustrated the idea of this radiation dosimeter is based on the shift in the PBG when it is exposed to gamma-ray radiation. Physically, this shift is due to the refractive index of doped PVA-Polymer depending on the γ-doses (in Gy unit). Therefore, the refractive index of PSi-layers is changed when exposed to γ-doses. The novelty of this pepper lies in the fact that this radiation dosimeter achieved a high sensitivity of 186 nm/RIU

Table 2 A comparison between our design and previous radiation dosimeters

References	Sensitivity	Based on	The materials used for detection
Kim et al. (2014)	0.011 dB/m·Gy	Co/Fe Co-Doped Alumino -Silicate Optical Fiber	0.011 dB/m·Gy
Mahdiraji et al. (2015)	0.232 (μC/mg·Gy)	Collapsed-Hole Ge-Doped Photonic Crystal Fiber	Ge-doped preforms
Entezam et al. (2016)	6.13–25.3 (nC/mg/Gy)	The thermoluminescence (TL) response of doped SiO(2) optical fibers	Al- and Ge-doped silica fibers
Cai et al. (2017)	None	pure-silica-core photonic crystal fibers (PSC-PCFs)	PSC-PCF samples
Raouafi et al. (2018)	None	Nickel-doped poly vinyl alcohol (PVA) films	(PVA/Ni2+)
Canning, et al. (2018)	None	Photonic Crystal Fiber Bragg grating (PCF-FBG) sensors	Germania-doped fiber
Ali Omer and Ali Bashir (2018)	0.06 (arb. unit) at 1 Gy	PVA/Cu_2O composite films	PVA/Cu_2O
Baccini, et al. (2019)	10 pm/ °C at 1550 nm	Optical Fiber Bragg Grating Sensors	Ge Doped fiber
Ibrahim et al. (2021)	150 (nm/RIU)	2D-PhC	PVA/CV + CF
Osman, et al. (2021)	None	PVA\$AgNO_3$ films	PVA\$AgNO_3$
This work	185, 195 (nm/RIU)	1D-PhC based on PSi layers	PVA/CV + CF

with very stability along of the range of visible wavelengths when the design is exposed to gamma-ray doses from 0 to 70 Gy. Furthermore, the effects of the thickness of the PSi-layers are studied to achieve the highest sensitivity. To the author's knowledge, this is the first time 1D-PhC based on PSi-layers has been used as a gamma-ray dosimeter. Finally, the other purpose of this radiation dosimeter is to be used as radiation-resistant FBGs for usage in nuclear environments in temperature and strain measurement applications.

Funding Open access funding provided by The Science, Technology & Innovation Funding Authority (STDF) in cooperation with The Egyptian Knowledge Bank (EKB).

Data availability Requests for materials should be addressed to Arafa H. Aly.

Code availability Requests for materials should be addressed to F. Sayed

Declarations

Conflict of interest The authors declare they have no conflicts of interest.

References

Abadla, M.M., Elsayed, H.A., Mehaney, A.: Novel design for the temperature sensing using annular photonic crystals. Silicon **13**(12), 4737–4745 (2021)

Abohassan, K.M., Ashour, H.S., Abadla, M.M.: A 1D binary photonic crystal sensor for detecting fat concentrations in commercial milk. RSC Adv. **11**(20), 12058–12065 (2021)

Afifi, M., et al.: Dosimetric impact of some gamma radiation-induced polymeric materials incorporated silicate using thermoluminescence and ultrasonic techniques. SILICON **14**(8), 4391–4400 (2021)

Ahmed, A.M., Mehaney, A.: Ultra-high sensitive 1D porous silicon photonic crystal sensor based on the coupling of Tamm/Fano resonances in the mid-infrared region. Sci. Rep. **9**(1), 1–9 (2019)

ALASIA, Dario, et al.: Study of the radiation effects on the properties of Brillouin scattering in standard Ge-doped optical fibres. In: 17th International Conference on Optical Fibre Sensors. SPIE, p. 180–183 (2005)

Ali Omer, M.A., AliBashir, E.A.: Synthesis of polyvinyl alcohol and cuprous oxide (PVA/Cu2O) films for radiation detection and personal dosimeter based on optical properties. J. Radiat. Res. Appl. Sci. **11**(3), 237–241 (2018)

Al-Syadi, A., et al.: Immersion-plated palladium nanoparticles onto meso-porous silicon layer as novel SERS substrate for sensitive detection of imidacloprid pesticide. Sci. Rep. **11**(1), 1–14 (2021)

Al-Kadhemy, M.F.H., Abass, W.: Optical properties of crystal violet doped PMMA films. Res. Rev. Polym. **4**(2), 45–51 (2013)

Aly, A.H., Mehaney, A., Eissa, M.F.: Ionizing particle detection based on phononic crystals. J. Appl. Phys. **118**(6), 064502 (2015)

Aly, A. H., Mohamed, D.: BSCCO/SrTiO3 One Dimensional Superconducting Photonic Crystal for Many Applications. J Supercond . Nov Magn 18, 1699–1703 (2015)

Aly, A.H., Sayed, F.A.: THz cutoff frequency and multifunction Ti2Ba2Ca2Cu3O 1 0/Ga As photonic bandgap materials. Int. J. Mod. Phys. B **34**(10), 2050091–20500913 (2020)

Aly, A.H. et al.: THz transmittance in one-dimensional superconducting nanomaterial-dielectric superlattice. Materials Chemistry and Physics 113, 382–384 (2009)
Ameen, A.A., Elsayed, H.A., Alamri, S., Matar, Z.S., Al-Dossari M, Aly, A.H.: Towards Promising Platform by Using Annular Photonic Crystals to Simulate and Design Useful Mask. Photonics. 8(9), 349 (2021)
Andreo, P., et al.: Fundamentals of ionizing radiation dosimetry. Wiley (2017)
Antar, E.M.: Effect of γ-ray on optical characteristics of dyed PVA films. J. Radiat. Res. Appl. Sci. **7**, 129–134 (2014)
Archer, J., et al.: High spatial resolution scintillator dosimetry of synchrotron microbeams. Sci. Rep. **9**(1), 1–7 (2019)
BACCINI, Desmond, et al. Gamma irradiation response in photonic crystal and standard optical fiber Bragg grating sensors for radiation dosimetry. In: AOS Australian Conference on Optical Fibre Technology (ACOFT) and Australian Conference on Optics, Lasers, and Spectroscopy (ACOLS) 2019. p. 27–28. SPIE (2019)
Bijalwan, A., Singh, B.K., Rastogi, V.: Analysis of one-dimensional photonic crystal based sensor for detection of blood plasma and cancer cells. Optik **226**, 165994–1659913 (2021)
Cai, W., et al.: Gamma-radiation effects in pure-silica-core photonic crystal fiber. Chin. Phys. B **26**(11), 114211–114219 (2017)
Canning, J., et al.: Gamma irradiation effects in photonic crystal fibre Bragg gratings. In: Australian Institute of Physics (AIP) Congress. (2018)
Chandrappa, H., et al.: Physico-chemical properties of PVA-Nile blue (C20H20ClN3O) polymer composite structures for γ-ray protection: a comparative γ-ray irradiation studies. Radiat. Phys. Chem. **184**, 109481–1094812 (2021)
Chmielewska, D.: Radiation methods and uses in nanotechnology. In: Sun, Y., Chmielewski, A.G., (eds.) Applications of Ionizing Radiation in Materials Processing, pp. 395–414 (2017)
Chu, R., et al.: Dosimetry systems for use in radiation processing: contents. J. ICRU **8**(2), NP-NP (2008)
Cocorullo, G., et al.: Measurement of the thermo-optic coefficient of a-Si: H at the wavelength of 1500 nm from room temperature to 200 °C. J. Non-Cryst. Solids **299**, 310–313 (2002)
Elsayed, H.A., Sayed, F.A., Aly, A.H.: Graphene deposited liquid crystal and thermal sensitivity using photonic crystals. Phys. Scr. **96**(3), 035503 1–12 (2021)
El-Shemy, S., et al.: Production of intensifying blue light by Cherenkov radiation phenomena and its application as a power source. Opt. Quant. Electron. **54**(2), 1–16 (2022)
Entezam, A., et al.: Thermoluminescence response of Ge-doped cylindrical-, flat-and photonic crystal silica-fibres to electron and photon radiation. PLoS ONE **11**(5), e0153913 1–15 (2016)
Hadi Al-kadhemy, M.F., et al.: The effect of (He–Ne) laser irradiation on the optical properties of methyl orange doped PVA films. J. Radiat. Res. Appl. Sci. **7**(3), 371–375 (2014)
Ibrahim, M.S.S., et al.: Highly sensitive photonic crystal gamma ray dosimeter. Opt. Quant. Electron. **53**(7), 1–19 (2021)
Ivanov, I., Skryshevsky, V., Belarouci, A.: Chemical sensor based on the colorimetric response of porous silicon photonic crystal. Sens. Actuators, A **333**,113309 1–14 (2022)
Iwamoto, S., Ota, Y., Arakawa, Y.: Recent progress in topological waveguides and nanocavities in a semiconductor photonic crystal platform. Opt. Mater. Express **11**(2), 319–337 (2021)
Kashaykin, P.F., et al.: Radiation-induced attenuation in silica optical fibers fabricated in high O2 excess conditions. J. Light. Technol. **33**(9), 1788–1793 (2015)
Kashaykin, P., et al.: Radiation induced attenuation in pure silica polarization maintaining fibers. J. Non-Cryst. Solids **508**, 26–32 (2019)
Kim, Y., et al.: Gamma-ray irradiation-induced optical attenuation in Co/Fe Co-doped alumino-silicate optical fiber for dosimeter application. J. Light. Technol. **32**, 4393–4399 (2014)
Mahdiraji, G.A., et al.: Collapsed-hole Ge-doped photonic crystal fiber as a diagnostic radiation dosimeter. J. Light. Technol. **33**(16), 3439–3445 (2015)
Mehaney, A.: Phononic crystal as a neutron detector. Ultrasonics **93**, 37–42 (2019)
Mehaney, A., Eissa, M.F., Aly, A.H.: Detection and discrimination between alpha particles and protons based on phononic crystals materials. Surf. Rev. Lett. **26**(07), 1850219 1–7 (2019)
Mir, F.A., Gani, A., Asokan, K.: Gamma irradiation studies of composite thin films of poly vinyl alcohol and coumarin. RSC Adv. **6**(2), 1554–1561 (2016)
Okada, Y., Tokumaru, Y.: Precise determination of lattice parameter and thermal expansion coefficient of silicon between 300 and 1500 K. J. Appl. Phys. **56**(2), 314–320 (1984)
Osman, I.M., et al.: Effects of additive and gamma irradiation on the structural and optical properties of polyvinyl alcohol doped with silver nitrate. GSJ. **9**(6), 1780–1792 (2021)

Park, H., et al.: Non-abelian charged nodal links in a dielectric photonic crystal. ACS Photon. **8**(9), 2746–2754 (2021)
Qutb, S.R., Aly, A.H., Sabra, W.: Salinity and temperature detection for seawater based on a 1D-defective photonic crystal material. Int. J. Mod. Phys. B **35**(01), 2150012 1–13 (2021)
Raghuvanshi, S., et al.: Effect of gamma irradiation on the optical properties of UHMWPE (Ultra-high-molecular-weight-polyethylene) polymer. Nucl. Instrum. Methods Phys. Res. Sect. B **271**, 44–47 (2012)
Raouafi, A., et al.: Effect of gamma irradiation on the color, structure and morphology of nickel-doped polyvinyl alcohol films: alternative use as dosimeter or irradiation indicator. Nucl. Instrum. Methods Phys. Res. Sect. B **425**, 4–10 (2018)
Rozaila, Z.S., et al.: Ge and B doped collapsed photonic crystal optical fibre, a potential TLD material for low dose measurements. Radiat. Phys. Chem. **126**, 9–13 (2016)
Sabra, W., et al.: Numerical optimization of 1D superconductor photonic crystals pressure sensor for low temperatures applications. Solid State Commun. **343**, 11467 1–8 (2022)
Sayed, H., et al.: Salinity sensor based on 1D photonic crystals by Tamm resonance with different geometrical shapes. Plasmonics **17**(1), 409–422 (2022)
Sharaf, F., et al.: The optical and mechanical properties before and after gamma irradiation of poly (vinyl alcohol) films doped with lead acetate. Polym. Degrad. Stab. **47**(3), 343–348 (1995)
Van, N.T., et al.: Select and rapid detection of methylene blue on porous silicon photonic crystals covered with silver nanoparticles by SERS. J. Electron. Mater. **51**(5), 1946–1949 (2022)
Wu, J.: Multichannel absorption enhancement in graphene based on metal-photonic crystal hetero-structure. ES Energy Environ. **13**, 25–30 (2021)
Yue, X., et al.: Porous silicon photonic crystal/silver composite produced by microwave-assisted reduction: applications to surface-enhanced Raman scattering. Opt. Mater. X **2**, 100027(1-5) (2019)
Zaky, Z.A., Aly, A.H.: Gyroidal graphene/porous silicon array for exciting optical Tamm state as optical sensor. Sci. Rep. **11**(1), 1–9 (2021)
Zhong, F., et al.: Optical characteristics of porous silicon photonic crystals prepared on the back surface of silicon wafers. Optik **201**, 163486 1–6 (2020)
Zimek, Z.: Application of radiation technologies for the modification of electronic devices. Institute of Nuclear Chemistry and Technology, 485–499 (2017)